DEVELOPMENT OF LABEL-FREE DETECTION SYSTEMS TARGETING FOOD-BORNE PATHOGENS

BY

ERIC MATTSON SALM

THESIS

Submitted in partial fulfillment of the requirements
for the degree of Master of Science in Bioengineering
in the Graduate College of the
University of Illinois at Urbana-Champaign, 2011

Urbana, Illinois

Advisers:

Professor Rashid Bashir
Assistant Professor Yong-Su Jin

Abstract

Food-borne pathogens and food safety-related outbreaks have come to the forefront over recent years. Estimates on the annual cost of sicknesses, hospitalizations, and deaths run into the billions of dollars. There is a large body of research on the subject of detection of food-borne pathogens, however, the widely accepted current systems are limited by high reagent costs, lengthy time to completion, and expensive equipment. This work has been developed with the goal of focusing on minimizing the time and reagent cost of two of the most common types of rapid, food-borne pathogen detection systems, i.e. immunoassays and real-time polymerase chain reaction assays. The first aim was to develop the proof-of-concept methodology for a label-free immunoassay technique utilizing photonic crystal biosensors targeting bacteria, specifically *E. coli* O157:H7. In this project, it is shown that detergent-lysing of the cells and extraction of their membrane antigens allows for the detection of down to 1E7 CFU/mL. Optimization of the blocking scheme takes the assay one step further and allows for specific detection of *E. coli* O157:H7 over *E. coli* K12. The second aim was to develop a label-free method for determining changes in DNA concentration as it relates to food-borne pathogen-targeted polymerase chain reaction assays. For this goal, impedance spectroscopy studies were carried out to characterize the system's capability in determining changes in concentration of purified DNA in DI water. To adequately measure the change in DNA concentration in a PCR solution, it was necessary to go through a purification and precipitation step to minimize the effects of primers, PCR reagents, and especially excess salts. It was shown that the purification and precipitation of the fully amplified PCR reaction showed a similar trend to the pure DNA in DI water characterization

tests. In developing the two versions of label-free detection systems, this work has brought cheaper, faster, smaller biosensors one step closer to reality.

Acknowledgements

I am grateful to a cooperative agreement with Purdue University and the Agricultural Research Service of the United States Department of Agriculture, project number 1935-42000-035 for funding Prof. Bashir at UIUC. I thankfully acknowledge Erich Lidstone, Dr. Brian Cunningham and SRU Biosystems for providing access and instruction on the BIND Reader and use of the photonic crystal platform. I sincerely thank Dr. Yi-Shao Liu for his contributions and guidance throughout completion of this work, and as a mentor during my first year in Dr. Rashid Bashir's lab. I would also like to thank my family and friends for their continued support throughout my professional and personal life.

I remain especially grateful for the sponsorship, guidance, and opportunity provided by my advisors, Dr. Rashid Bashir of the Electrical and Computer Engineering Department and the Bioengineering Department at the University of Illinois at Urbana-Champaign and Dr. Yong-Su Jin of the Food Science and Human Nutrition Department at the University of Illinois at Urbana-Champaign.

Table of Contents

Chapter 1. Introduction

1.1 Overview of the Problem

Food pathogens and food safety-related outbreaks have come to the forefront over recent years. From *Escherichia coli* O157:H7 in spinach to *Listeria monocytogenes* outbreaks in ready-to-eat deli meats, people have taken notice when it comes to keeping their food safe. The Center for Disease Control and Prevention (CDC) estimates that there are 47.8 million cases of food-borne illnesses every year in the United States alone. Among those cases, 127,839 resulted in hospitalizations and 1,686 people died [1]. In terms of financial costs, the CDC along with the USDA's Economic Research Service puts the cost of just *Salmonella*-related illnesses at ~$2.6 billion in 2009 [2]. When including *E. coli*, *L. monocytogenes*, and *Campylobacter* infections, this cost was found to be as high as $6.9 billion dollars in 2000 [3]. Given these numbers and the population's awareness of the problem, the field of food-borne pathogen research has never been deeper. Each scientific discipline has its own take on food-borne pathogen detection. From the purely electrical detection techniques of electrical engineers to the culture and serotype methods of microbiologists, new procedures covering different principles arise every year. The National Advisory Committee on Microbiological Criteria for Foods presents an excellent review of food-borne pathogen detection methods from rapid techniques to more traditional standards [4].

Although AOAC International, a non-profit, scientific accreditation association, has validated and certified more than 100 rapid pathogen testing kits, food scientists will still tell us that there is no replacement for the standard conventional techniques of cultural enrichment, selective

enrichment and eventual typing of the grown microorganism [5-6]. The gold standards of the industry are not going to go away overnight. They have proven themselves to be reliable, they are relatively simple, and they are inexpensive. Food scientists trust the results from standard techniques and are comfortable passing down an order for a recall based on the experiment's outcome. However, there are numerous reasons to try to find a better solution to the problem of pathogen detection. Primarily, the gold-standard conventional method takes time. Tests to determine the presence of a pathogenic serotype can take upwards of a week. In the realm of perishable foods, the food industry does not have the shelf-life to allow foods to sit for upwards of 7 days before shipment. The goal for any new method has to be to greatly diminish the time from obtaining the sample to end result.

Although the cost of lost time on the shelf is high with conventional techniques, the cost of growth and cultural serotyping assays remains low. The rapid techniques currently offered to the food industry such as immunoassays and real-time polymerase chain reaction (PCR) assays are hindered by increased cost of reagents and equipment that accompany the more advanced techniques. For the food industry to adopt a new methodology, the cost and reliability of the new assay must remain competitive with traditional procedures.

In the design of a perfect system, a scientist must take a food sample from the sample collection stage, through a pre-analytical processing step, into a analyte detection phase, all the way to data analysis, and some user output. Each of these steps is as important as the last. Each one provides its own unique challenges and limitations. Each individual step is a bottleneck that must be addressed and optimized before a complete rapid system can be implemented.

1.2 Current Pathogen Detection Systems

1.2.1 Immunoassays

Traditional immunoassays such as Enzyme-Linked Immunosorbant Serologic Assays (ELISA), though accepted as sufficient by food industry professionals and accreditation boards such as the AOAC, are not perfect and can be improved. As depicted in Figure 1, immunoassays rely on the use of secondary antibodies and enzyme-linked anti-secondary antibodies. The goal of a label-free system would be to eliminate the use of the secondary antibodies and enzymes in order to minimize the steps involved in the process while maintaining sensitivity and specificity.

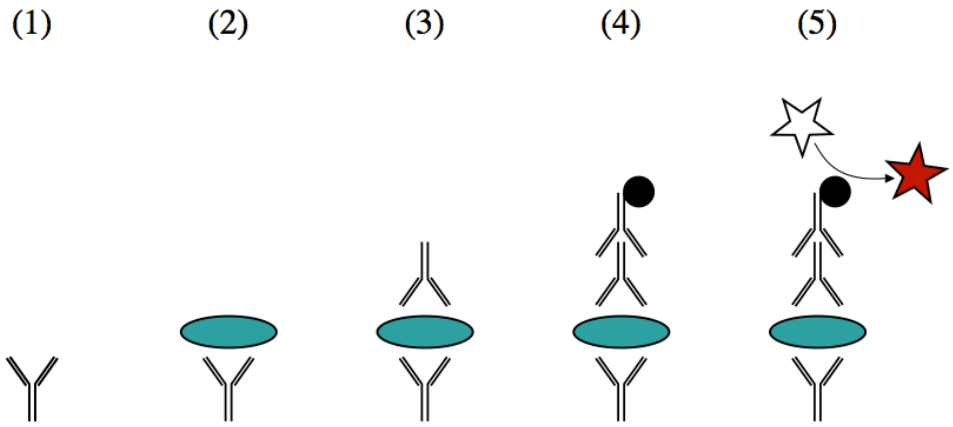

Figure 1: The methodology for the ELISA protocol is demonstrated. Step (1) involves binding of an antibody to the surface of a microplate. Step (2) shows a target analyte binding to the antibody and remains bound after a washing step. Step (3) represents a secondary antibody that is added to the solution that will bind to the bound analyte and will stay bound through a subsequent washing step. Step (4) shows an enzyme-linked anti-secondary antibody that binds to the anti-secondary antibody. Step (5) represents the enzyme catalyzing reaction that leads to a change in the overall solution characteristics such as color or fluorescence.

1.2.2 Real-time PCR

In 1992, the first end-point fluorescence detection of PCR amplification was published [7]. By incorporating an intercalating dye, ethidium bromide, that fluoresces more brightly when bound to double stranded DNA, scientists were able to detect changes in fluorescence intensity from the beginning to the end of the thermal cycling. In 1993, the first kinetic PCR analysis was demonstrated (see Figure 2) [8]. Together, these two papers paved the way for real-time PCR assays in modern science. However, usage of real-time PCR systems is limited by the added cost of fluorescent dyes such as SYBR green and also by the cost and size of the optical detection equipment that accompanies fluorescence-based assays. A system that eliminates the need for the fluorescent dye and subsequent optical detection equipment would greatly improve the field of real-time PCR.

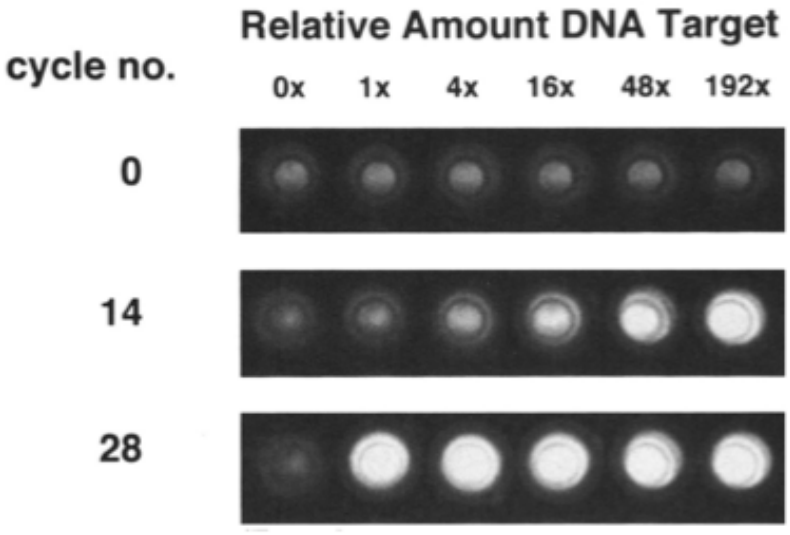

Figure 2: In Higuchi's pioneering paper in 1993. The potential for using intercalating dyes for real-time PCR assays was demonstrated. In this picture, the change in fluorescence intensity can be seen as a function of PCR cycle number and DNA concentration [8].

1.3 Scope of the Research

This thesis has been developed with the goal of focusing on minimizing the time and reagent cost of two of the most common types of rapid, food-borne pathogen detection systems, immunoassays and real-time polymerase chain reaction assays. The proposed detection methods exist within the analyte detection module of a complete food-borne pathogen detection system and are not meant to represent a perfect system, but rather, an example of how to address a bottleneck in immunoassay and real-time PCR systems.

1.4 Justification of the Study

Rising commodities prices mean that the food industry will be working with increased prices and tighter margins [9]. In order for food companies to remain competitive while maintaining quality, industry professionals must minimize or even eliminate excess costs. The development of more cost-efficient, reliable food-borne pathogen detection methods will enable food companies to provide safer food, faster at a more affordable cost to the consumer.

1.5 Goals

1.5.1 Specific aim 1

To develop the proof-of-concept methodology for a label-free immunoassay technique utilizing photonic crystal biosensors targeting bacteria, specifically E. *coli* O157:H7.

Photonic crystals offer a unique platform for bacterial detection. Their properties, as discussed further in chapter 2, allow for the detection of binding events at the sensor surface. By functionalizing a photonic crystal surface with a biorecognition element such as an antibody, it is possible to detect specific binding events as the bacterium of interest interacts and binds to the chosen antibody.

In the proposed label-free system, the method of detection relies only on the binding of the bacterial analyte to a biorecognition element at the surface of the sensor. The elimination of added reagents like the secondary antibody or the enzyme would advance the field of immunoassays and reduce the cost to the food industry.

1.5.2 Specific aim 2

To develop a label-free electrical method for determining changes in DNA concentration as it relates to food-borne pathogen-targeted polymerase chain reaction assays.

Polymerase chain reaction assays for bacterial detection are commonplace in laboratories. Traditionally, successful amplification of a target gene sequence was confirmed through gel electrophoresis. As gel electrophoresis takes upwards of an hour, it became necessary to develop a real-time method for confirming successful amplification. Fluorescent dyes that fluoresce at much greater levels when bound to double-stranded DNA were introduced to PCR systems in the early 1990s. These dyes such as SYBR green and EVA green allow scientists to detect amplification of a target sequence as it occurs.

However, fluorescence-based systems require complex optical excitation and detection devices, as well as the inclusion of often proprietary and expensive fluorescent dyes. By eliminating the need for optical detection and replacing fluorescence detection with electrical detection of DNA molecules in solution, researchers can reduce the footprint of a PCR system, the cost to run the system and still maintain the speed and reliability that food industry quality control demands.

Chapter 2. Development of a Photonic Crystal-Based Biosensor for Detection of E. *coli* O157:H7

This work was presented in a poster presentation session at the 2010 Institute for Food Technologist's Annual Meeting & Food Expo. in Chicago, IL.

2.1 Introduction

For food scientists, it is important to continually refine current detection methods, as well as develop new assays, in order to make sure the food industry has access to the fastest, most reliable procedures for pathogen detection. Minimizing cost and keeping sensors specific, fast, and sensitive should be the areas of focus for future developments in detection systems. To this end, the prospect of label-free detection systems is particularly interesting. Label-free systems minimize the number of reagents while cutting down on time by eliminating the steps associated with labeling. Photonic crystal systems that rely on label-free sensing have been extensively researched in recent years. These systems have been used to detect viruses, protein-protein interactions, small molecule interactions, cytotoxicity of compounds, and kinetic reaction rate constants [11-16]. In terms of bacterial detection, the only method demonstrated with photonic crystals is a scattering-based assay. In this method, cells are bound to the photonic crystal surface which causes light to scatter around the bacteria. This scattered light is then detected and its intensity related to the bacterial concentration [17]. The objective of this study was to develop a proof-of- concept method that utilizes photonic crystal biosensors (PC) for rapid,

label-free detection of *E. coli* O157:H7. For this study the biosensor's mechanism is based on changes in which wavelengths of light are reflected and not based on just scattering of light.

2.2 Method of Detection

A crystal is a periodic arrangement of atoms or molecules. A photonic crystal replaces the periodic arrangement of atoms with a periodic arrangement of materials with different indices of refraction. As electromagnetic waves interact with the photonic crystal, only certain wavelengths of light are allowed to pass through the crystal. As the indices of refraction change due to binding of materials to the photonic crystal surface, the wavelengths of light that are allowed to pass through the crystal will change. Mapping the change in which wavelengths are and are not allowed to pass through the crystal allows for direct observation of binding events at the photonic crystal surface [10]. A generalized schematic of the photonic crystal system used in this work is shown in Figure 3.

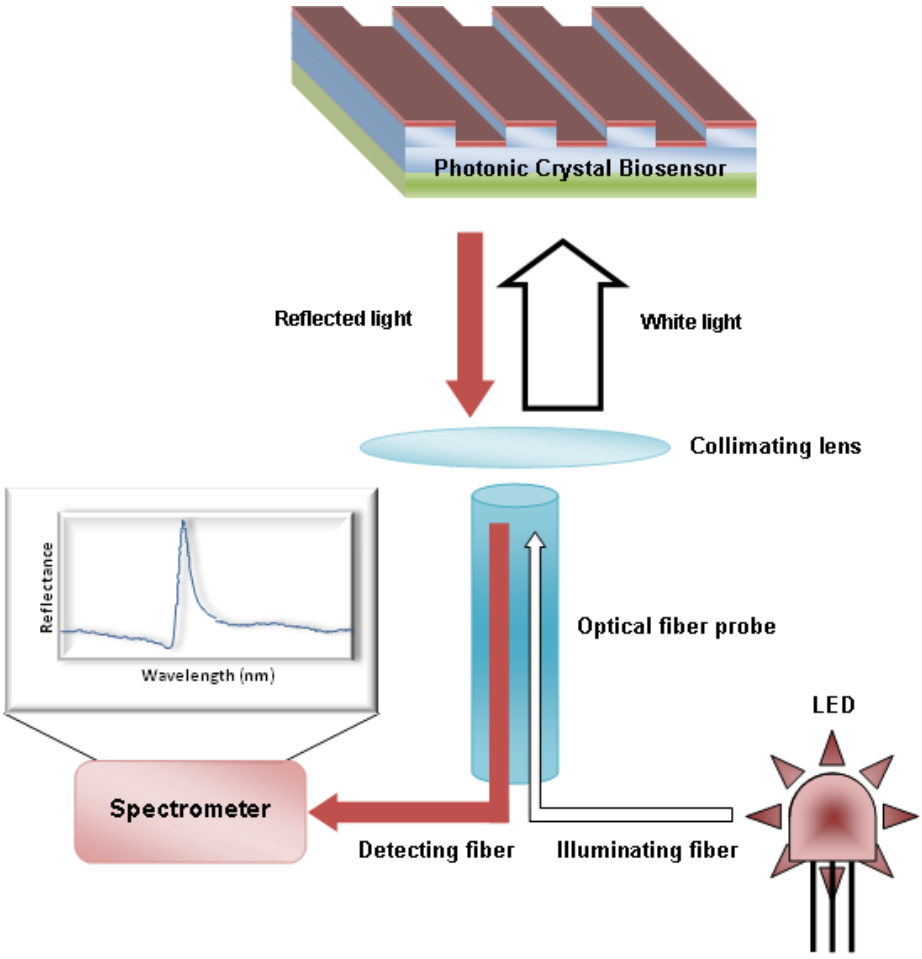

Figure 3: This demonstrates the general operating principles of the BIND Reader system. An optical fiber, with a broadband LED light source, passes light through a collimating lens and is incident to the sensor surface. Depending on the structure and surface properties of the photonic crystal, a certain bandwidth of wavelengths is reflected back off the sensor. This reflected light is collected by the optical fiber probe and the spectrum of wavelengths is determined using a spectrometer. The peak wavelength value is determined by looking for the wavelength with the greatest reflectance [11].

2.3 Materials

Streptavidin-coated photonic crystal 384-well plates obtained from SRU Biosystems (Woburn, MA) were used as the sensor to detect *E. coli* O157:H7. The platform used was the BIND Reader, also from SRU Biosystems. The polyclonal antibodies used were obtained from KPL and were chosen due to their low cross reactivity with other bacteria [18]. The antibodies were then biotinylated at the Immunological Resource Center at the University of Illinois at Urbana-Champaign to allow the antibodies to bind to the streptavidin-coated photonic crystal plates. The polyclonal antibodies were diluted down to their final concentration using PBS obtained from Sigma-Aldrich. The blocking agents used, casein blocker, SeaBlock, and Starting Block were obtained from Pierce Protein Research Products, a division of Thermo Scientific. The *E. coli* O157:H7 was maintained in LB media broth from Sigma-Aldrich in a 37°C incubator. 16-20 hours before each experiment, 100µL of *E. coli* O157:H7 was inoculated into 10mL of BHI broth and placed in the incubator for later use. For the cell lysis and protein extraction, Bacterial Protein Extraction Reagent or B-PER was obtained from Pierce Protein Research Products.

2.4 Methods

E. coli O157:H7 was specifically detected through the use of polyclonal, biotinylated-anti *E. coli* O157:H7 antibodies bound to the photonic crystal surface using steptavidin-biotin linkage chemistry. To prepare the sensor, each well was rinsed three times with 100µL of distilled, ionized water (DI). Each well was then filled with 50µL PBS and allowed to equilibrate until the readings from the BIND system stabilized. After the peak wavelength value for each well

stabilized, depending on the experiment, wells were coated with 50µL of 50µg/mL of biotinylated polyclonal antibodies and allowed to incubate for 1 hour on a shaker plate. The antibody solution was then removed and the sensor again washed three times with DI. Each well was then filled with 50µL of PBS and the peak wavelength value was recorded using the BIND System. Once this reading stabilized, the appropriate blocker was added to each well. Depending on the experiment, 50µL of either casein, Sea Block or Starting Block was pipetted into each well. The blocker was allowed to sit for 1 hour in an incubator on a shaking plate. After the well was coated with the antibody and the selected blocker, it was exposed to 35µL of either whole *E. coli* O157:H7 or *E. coli* O157:H7 cells that had been detergent-lysed with B-PER for 15 minutes. After one hour in the incubator on a shaking plate, the wells were again washed three times with 100µL of DI and then filled with 50µL of PBS. The sensor was then placed in the BIND System and the peak wavelength value recorded and the change in peak wavelength value from the previous step noted.

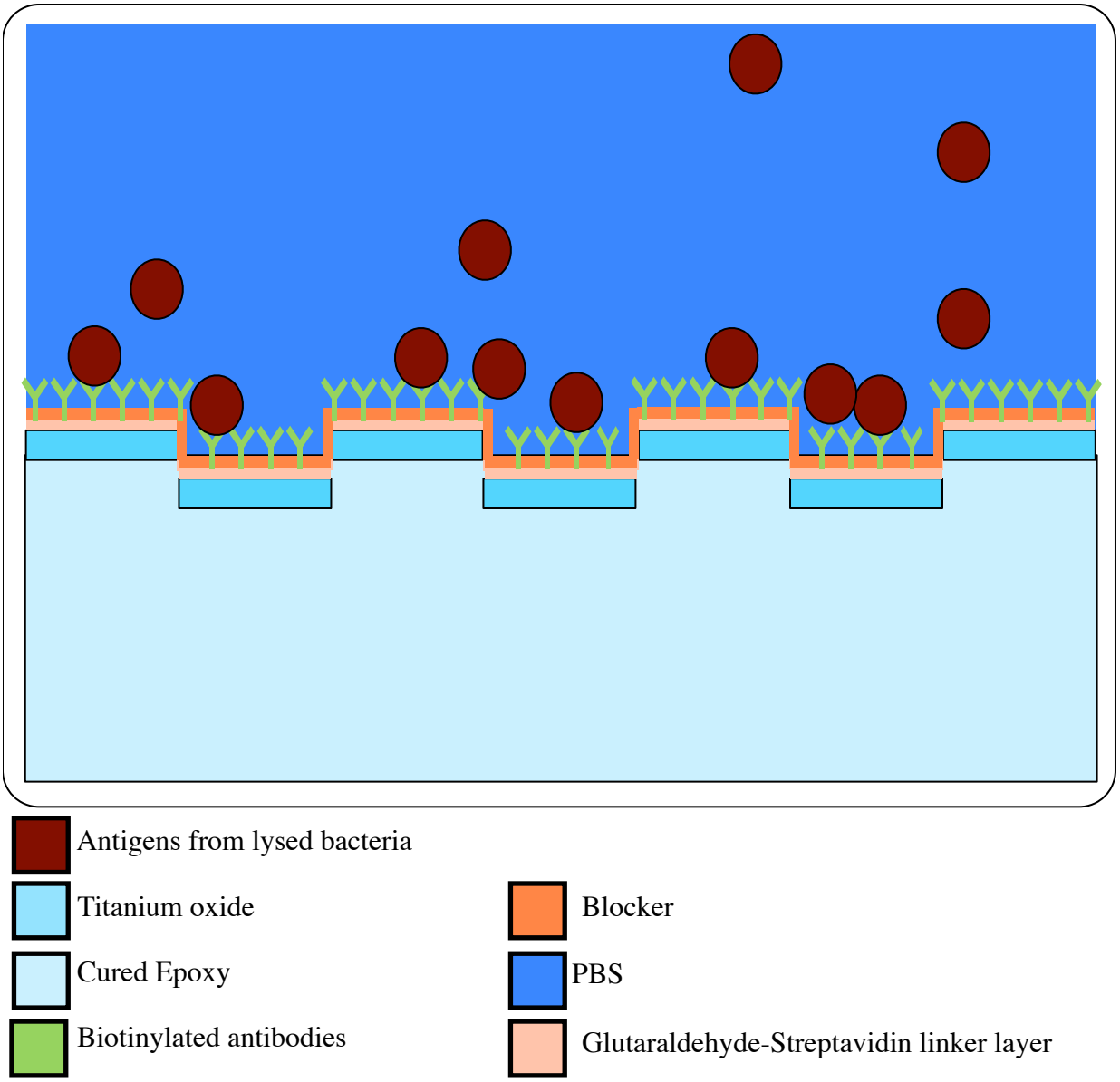

Figure 4: Schematic of the sensor showing biotinylated antibodies bound to a streptavidin linker layer on a titanium oxide surface. A blocker layer is utilized to minimize non-specific adsorption. The target antigen binds to the exposed antibodies, resulting in a change in local refractive index. This change is measured using the BIND Reader by examining the peak wavelength shift for the well and how it changes from before to after adding analyte.

2.5 Results/Discussion

The addition of antibodies to the photonic crystal surface is of utmost importance. Obtaining a high enough antibody density on the photonic crystal surface will increase the likelihood that an antigen interacts with the antibodies when the antigen approaches the sensor surface. Antibodies were added to the streptavidin-coated plate at varying concentrations, 100 μg/mL, 50μg/mL, and 10μg/mL. It was found that the peak wavelength shift saturated at 50μg/mL and above (data not shown). For 10 μg/mL, the shift induced was greatly diminished. Setting a point of 50μg/mL allows for high antibody binding density while maintaining the lowest possible sensor cost.

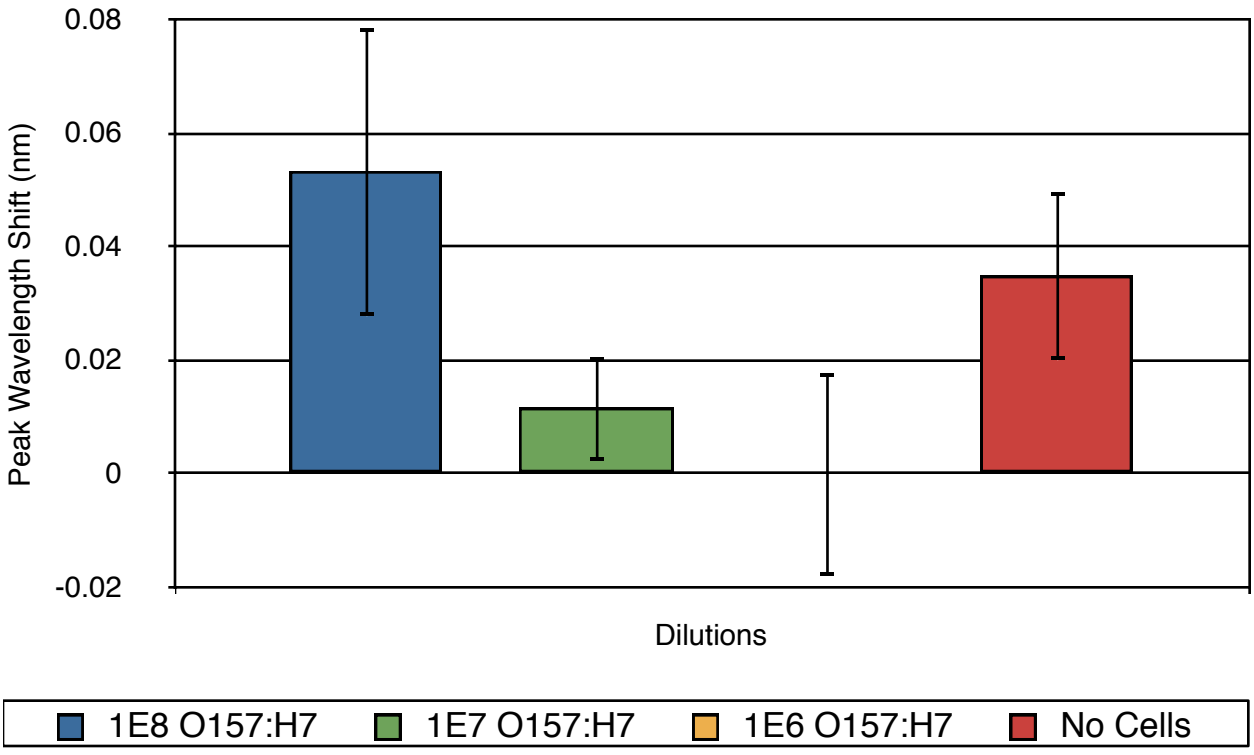

Figure 5: Detection of whole cells with the current version of our biosensor was limited. The peak wavelength shift from 1E8 CFU/mL is functionally indistinguishable from the control well that contained no cells.

Figure 5 shows that the 384-well photonic crystal sensor was unable to detect the highest tested concentration, 1E8 CFU/mL of *E. coli* O157:H7. This is likely because either our concentration of analyte was too low, there existed a diffusion limitation of whole cells in the well, or the whole cells that were bound to the antibodies did not greatly affect the local refractive index at the sensor surface and induce a large peak wavelength shift. As the *E. coli* culture had already reached its carrying capacity, getting a higher concentration of our analyte was not attempted. Altering the rate at which the analyte diffuses and interacts with the antibodies as well as maintaining similarity with the known-to-work antibody addition experiment was the chosen option for troubleshooting. To this end, the breakage of cells into many pieces coupled with a membrane protein extraction was attempted in order to detect a smaller number of initial target cells.

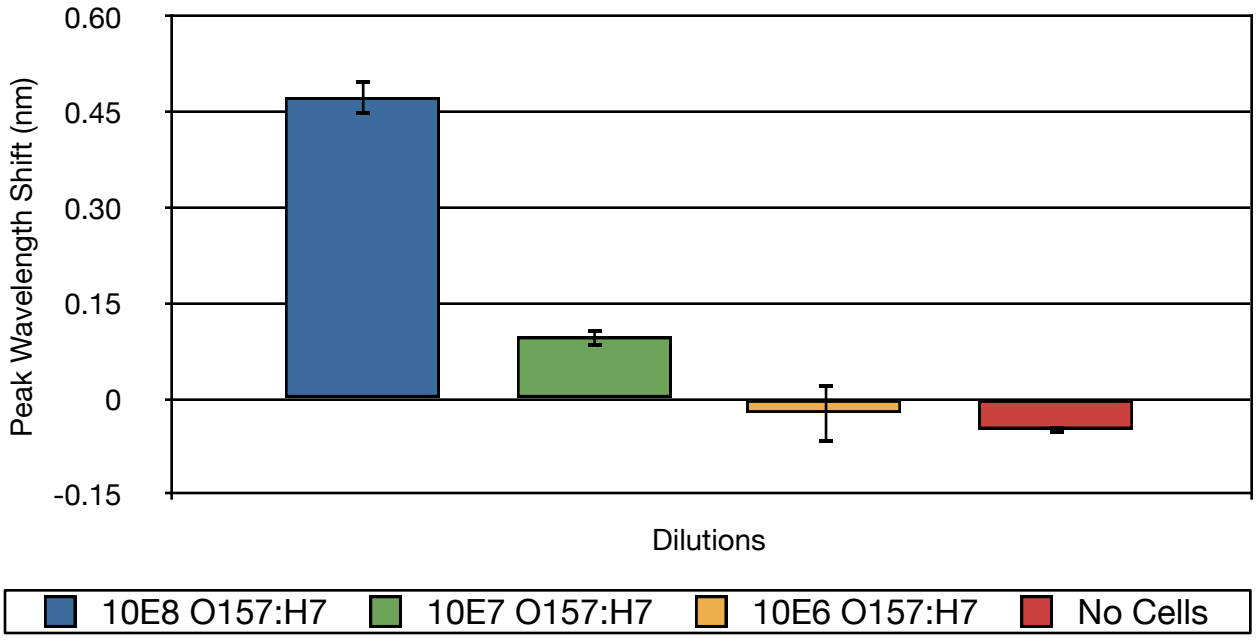

Figure 6: Peak wavelength shift values for varying concentrations of detergent lysed, membrane protein extracted *E. coli* O157:H7 was examined.

Through lysing the cells with B-PER and extracting the membrane proteins, the size of the analyte being detected was diminished. This increases the rate of diffusion and thus, the likelihood that the bacteria's surface protein antigens would interact with the polyclonal antibodies. Lysing the bacterium also increases the number of independent antigens in solution which might play a role in the increased level of detection. Our experimental results, see figure 6, using lysed cells show that there is a distinguishable difference between 1E8 CFU/mL and 1E7 CFU/mL and the control well without cells. A similar increase in the limit of detection from detergent lysing and protein extraction was reported in the case of a biosensor employing a flow-through SPR detection method [19]. However, no such experiment has been done using a photonic crystal biosensor in a static well with bacteria.

The next step taken in development of this biosensor was to determine the specificity of the assay. The *E. coli* O157:H7 antibodies used are known to have little cross-reactivity with other bacteria, however, non-specific adsorption of non-target analytes to the sensor surface will induce a peak wavelength shift. In this regard, it is necessary to optimize the blocking of the sensor surface. Figure 7 shows the resulting peak wavelength shifts when three common blocking agents are used. The figure also demonstrates the shift induced by non-specific adsorption when *E. coli* K12 is added to the sensor surface. The non-specific adsorption of *E. coli* K12 to the sensor surface is very high. For both the Sea Block and the Starting Block, the shift from K12 vs. O157:H7 are almost functionally indistinguishable. However, the casein blocker provides much better blocking to K12 without inhibiting the binding of O157:H7. To quantify the quality of blocking, an efficacy of blocking parameters was designed (see Figure 8). This parameter compares the shift induced by 1E8 O157:H7 vs. the shift from 1E8 K12. A lower

ratio is desired due to the O157:H7 shift being placed in the denominator. Sea Block and Starting Block show efficacy of blocking parameters near 0.8 whereas casein sits much lower at less than 6. This experiment helps demonstrate the difference in blocking between the different agents with casein being around 25% better at blocking non-specific adsorption.

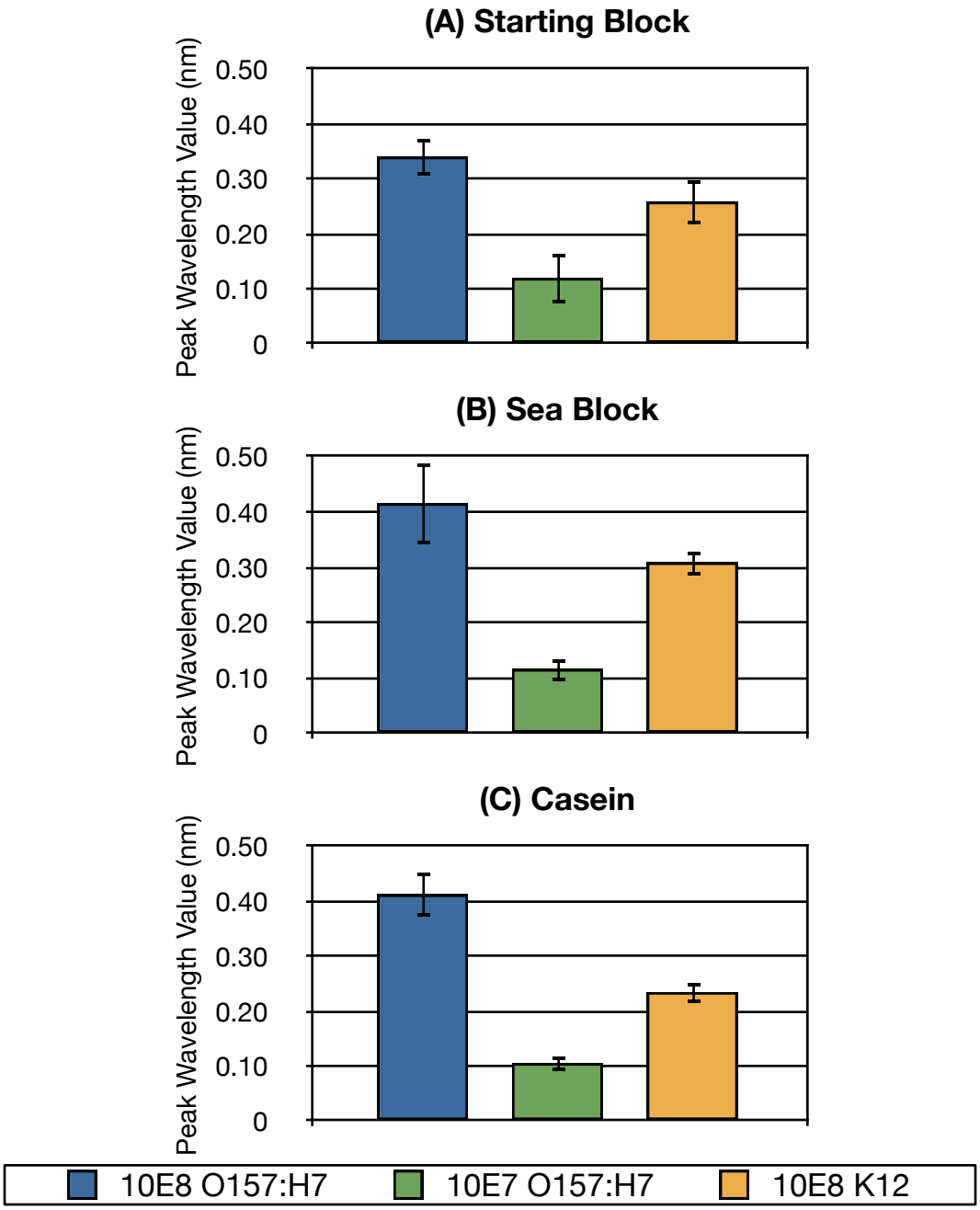

Figure 7: Non-specific binding of cellular debris on the surface of our biosensor seems to have caused the measured low signal-to-noise ratios. Optimization of blocking protocols by adding a further surfactant-based washing treatment as well as attempting different blockers resulted in a much higher signal-to noise ratio.

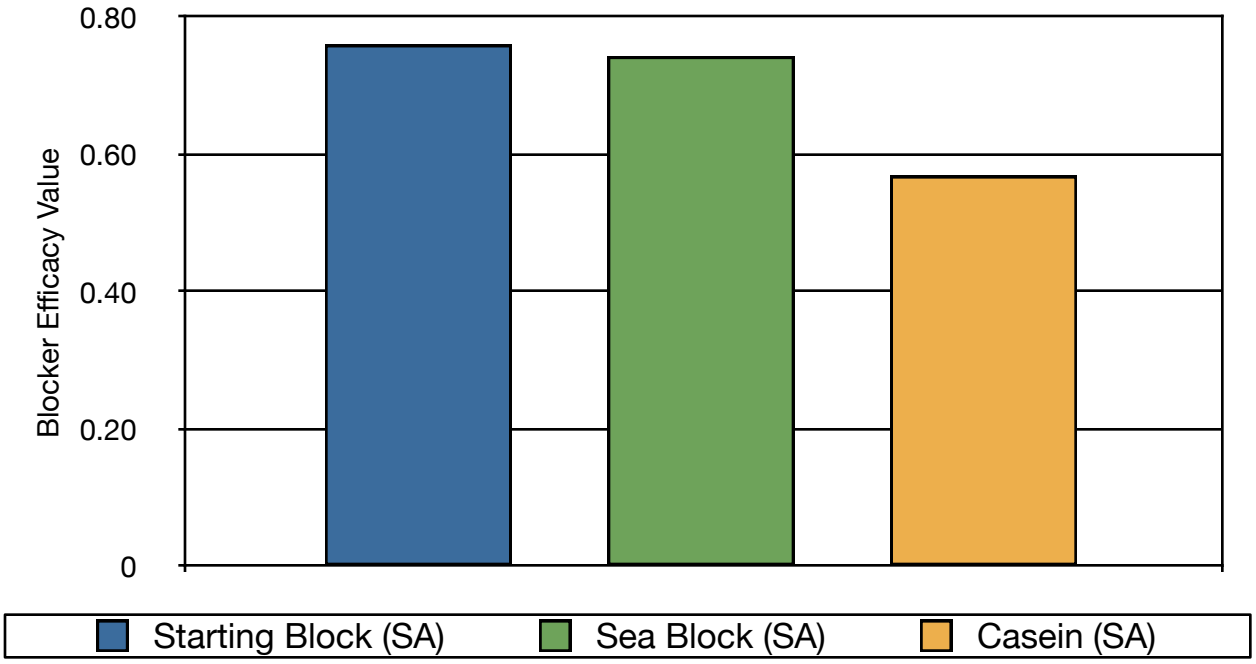

$$\text{Blocker efficacy} = \frac{\text{PWS(1E8 K12)}}{\text{PWS (1E8 O157:H7)}}$$

Figure 8: Blocking efficacy of Starting Block, Sea Block and casein were investigated. Casein on the streptavidin-coated plate provided the best blocking characteristics.

2.6 Conclusions

This study details the initial stages of development of a label-free, PC-based biosensor capable of detecting bacterial cells in solution. While the current detection limit of this system is relatively high, further development of the assay could put this system above other immuno-based detection methods such as ELISA while minimizing cost due to the assay's label-free protocol. Through this method, the developed PC sensor was able to detect 1E7 CFU/mL of *E. coli* O157:H7 and certain blockers were shown to have different blocking efficacies.

Chapter 3. Electrical Detection of dsDNA and the Application of Polymerase Chain Reaction Amplification Detection

3.1 Introduction

Since the inclusion of thermostable DNA polymerases from *Thermus aquaticus* in 1988, polymerase chain reaction assays have become commonplace in labs [20]. Overcoming the requirement to add fresh polymerase after each thermal cycle greatly improved the time, labor, and cost of PCR. By 1992, the first end-point fluorescence detection of PCR amplification was published [7]. By incorporating an intercalating dye, ethidium bromide, which fluoresces more brightly when bound to double stranded DNA, scientists were able to detect changes in fluorescence intensity from the beginning to the end of the complete thermal cycling process. In 1993, the first kinetic PCR analysis was demonstrated [8]. In this experiment, a video camera monitored changes in fluorescence over the course of thermal cycling. Together, these three papers paved the way for real-time PCR assays in modern science.

In 1993, Northrup et al. reported the first micro-fabricated reaction chamber for DNA amplification [1]. Micro-fabrication technologies have enabled the realization of portable PCR systems by significantly reducing the thermal mass by utilizing miniaturized reaction chambers. The size of these on-chip chambers range from micro [22-26] to sub-nano liter scale [27]. These developments have not only made rapid heating and cooling ramp rates possible for fast, efficient PCR, but can also save a significant amount of samples, reagents, and workspace.

However, a portable and fast PCR machine for point-of-care and on-site diagnosis will not be practical without a simpler detection method than fluorescence for the amplified PCR products. As of today, the state of the art micro-fabricated devices focus mainly on two detection methodologies, an optical detection approach, such as on-chip capillary electrophoresis detection [8-10] or labeling the amplified products with fluorescent dye and reporter particles for detection [11-12], and an electrochemical approach using either complementary probe binding [33-34] or surface charge sensing [35]. Although, these methods are rapid in comparison to the conventional gel electrophoresis methods; the requirement of an optical component integrated into micro-fabricated devices with respect to the optical method, or a functionalized surface for DNA hybridization for the electrochemical method, not only limits the mobility of such devices, but also increases the labor and total cost of operation.

Instead of using a fluorescence label for optical detection or a oligomeric probe for electrochemical detection, the electrical properties of DNA molecules first researched back in 1950's and 1960's [36-39] are a good candidate for developing a novel, simpler PCR detection method. In this study, the change in impedance and phase with respect to changing DNA concentration was interrogated to demonstrate a novel PCR detection method.

3.2 Method of Detection

It has been shown that, in solution, DNA molecules, due to their negatively charged sugar-phosphate backbone, will be surrounded by a counter-ion cloud [40] These counter-ions are usually classified as two layers; one is associated with bound ions, i.e. condensed ions closed to

the DNA molecule while the other layer is a loosely surrounding ion cloud. The two separate counter-ion layers give rise to two different dielectric relaxation points when the DNA molecules are probed in an AC electrical field over a range of frequencies [41-42] Tomic et al. discussed the mechanisms for the lower frequency dielectric relaxation point in low salt concentrations in great detail [43]. As depicted in Figure 9, the dielectric dispersion is a function of the condensed ion cloud fluctuating between the ends of the DNA molecule in an end-to-end movement. As the measurement frequency increases, the DNA and its surrounding cloud are not able to align with the electric field quickly enough, resulting in a dielectric relaxation point in the system. At higher frequencies, the closely bound condensed ion layer forms a dipole with the negatively-charged phosphate groups of the DNA backbone which introduces another dielectric relaxation point related to the DNA molecule's axial rotation.

Due to the complexity of the different types of background ions, charge neutralization and binding to the back-bone in highly ionic solutions, such as PCR reagent, it is necessary to purify and resuspend the PCR product in DI water. In prior work, it was shown that increasing the DNA concentration will increase the effect of the induced dipole moments [44]. Therefore, as the effect of the induced dielectric relaxation point increases and measured impedance and phase of the system changes, it is possible to conclude that the concentration of dsDNA in the system is increasing and that PCR amplification is occuring.

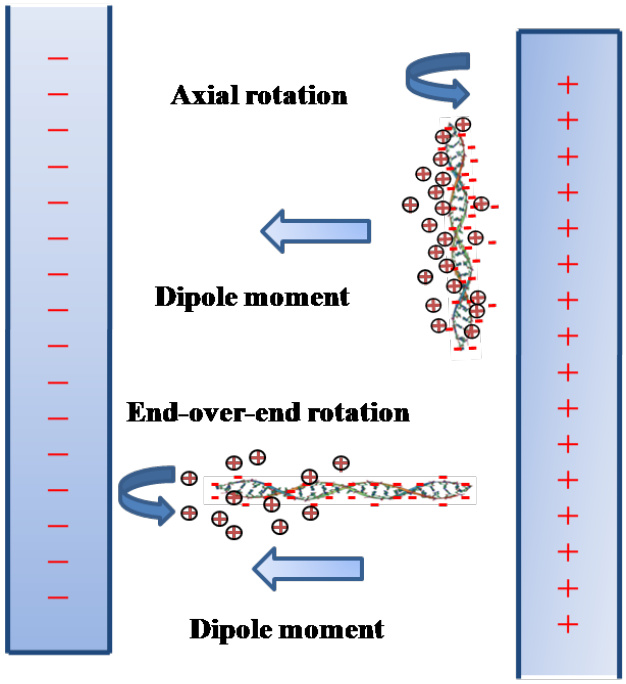

(a)

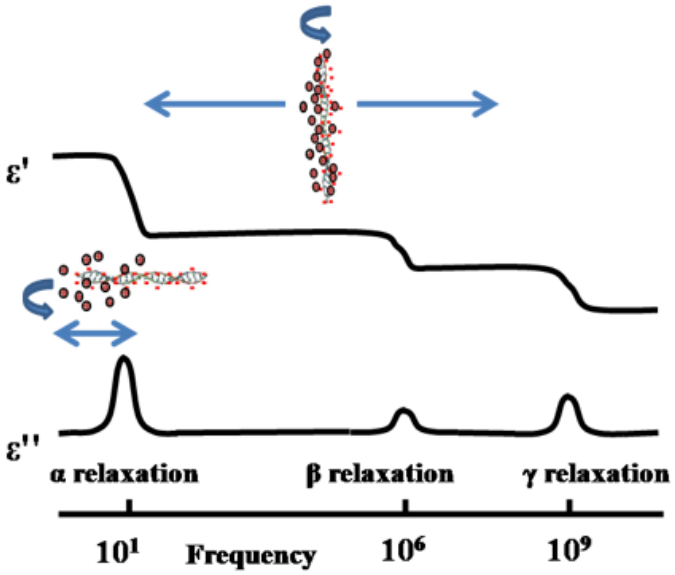

(b)

Figure 9: Three dielectric relaxation points are known to exist for DNA. The first point is in the low frequency range and corresponds to end-to-end rotation. The second point is in the 100kHz-1MHz range and corresponds to axial rotation. The final relaxation point falls above 1GHz and corresponds to the orientational polarizability of water molecules surrounding the DNA molecules.

3.3 Materials

Listeria monocytogenes was grown in Brain Heart Infusion broth from Sigma Aldrich. PBS was also obtained from Sigma Aldrich. Nuclease-free water for the resuspension of primers and DNA was obtained from Ambion, Inc. Ready-to-go PCR beads were obtained from GE Healthcare Life Sciences. A Qiaquick PCR purification kit from Qiagen, Inc. was used in the PCR preparation. For the alcohol precipitation procedure, ammonium acetate, isopropanol, and ethanol were obtained from Sigma Aldrich. The 100, 500, and 5000bp DNA fragments were purchased from the NoLimits line of DNA at Fermentas Molecular Biology Tools, a division of Thermo Scientific Inc. Primers for the prfA gene were purchased from Integrated DNA Technologies, Inc. All centrifugation steps were performed in a Centrifuge 5415D from Eppendorf). DNA sample purity was interrogated using a Nanodrop spectral photometer (Nanodrop, Wilmington, DE). Injection of the sample into the microchip was accomplished using a PHD ULTRA syringe pump from Harvard Apparatus. The microchip sensors (see Figure 11) and LCR meter used were provided by BioVitesse Inc (San Jose, CA).

3.4 Methods

3.4.1 DNA Precipitation

The 100, 500, 5000 base pair DNA molecules were prepared using an isopropanol precipitation technique. Equal volume of ammonium acetate was added to the DNA followed by three times the initial volume of isopropanol. This solution was vortexed on a table-top vortex and let to sit

in -20°C freezer for 5 hours to ensure precipitation. The samples were then loaded into a centrifuge and centrifuged at room temperature for 25 minutes at 14000g. The supernatant was then removed and the tube was washed with 1mL of 95% ethanol by inverting the tube several times and left to sit on ice for 10 minutes. The samples were the centrifuged again at 14000g for 15 minutes and the ethanol supernatant pipetted off the DNA pellet. The tube was then left to air dry to remove any left-over ethanol for 30 minutes. Once dry, the DNA molecules were resuspended in nuclease-free de-ionized water and diluted down to the desired concentrations. The purity of the DNA samples was confirmed by a spectrophotometer, by examining the A260/ A280 ratio which must fall between 1.8 and 2.0 for pure DNA (Nanodrop, Wilmington, DE).

3.4.2 PCR samples

All the samples were prepared from *Listeria monocytogenes* cultures that were incubated for 18-20 hours in BHI broth in a 37°C incubator. One mL of cell culture was collected and heat lysed in a 95°C water bath for 15 minutes, followed by 5 minutes quench in a -20°C freezer. Following cell lysis, the cellular debris was spun down at 15000g for 30 seconds in a centrifuge. The supernatant was then collected and checked for purities and concentrations by a Nanodrop spectral photometer (Nanodrop, Wilmington, DE).

PCR sample preparation was accomplished using three, 25µL Ready-to-go PCR beads for each cycle sample. To obtain a view of the reaction kinetics, 0, 10, 20, 30 and 40 cycles will be measured. To generate the PCR samples for each cycle sample, an initial stock of 16 beads was used to eliminate pipetting errors between cycle samples. Initially 352µL nuclease free DI water was added to rehydrate the lyophilized beads, followed by 8µL of 10µM forward and 8µL of

10μM reverse primers to get a final primer concentration of 0.1μM. Finally, 32μL of template solution was added to the stock solution. From this point, 75μL was pipetted into 5 individual tubes for the 0, 10, 20, 30, 40 cycle measurements. Left-over solution was put in a second 40 cycle tube that would be used to confirm successful PCR amplification through gel electrophoresis.

The forward and reverse primers used for the PCR reaction targeted the *L. monocytogenes* prfA gene, which is a protein that positively regulates *Listeria monocytogenes* virulence factors:

LMPRFA-F CGGGATAAAACCAAAACAATTT (5′ to 3′)

LMPRFA-R TGAGCTATGTGCGATGCCACTT (5′ to 3′)

Samples of designated cycles for each replicate were prepared with all the templates, primers and PCR reagents mixed well before distributing to each PCR reservoir. Two negative controls consisting of samples without primers and samples without template were made in order to rule out effects from just the primers and just the template.

The PCR was performed with a pre-heat step of 94°C for 2 minutes. This ensured that the genomic DNA molecules were completely denatured. The amplification process consisted of 40 cycles with each cycle containing three steps: 30 seconds at 94C for denaturation, 30 seconds at 55°C for annealing, and 30 seconds at 72°C for extension. At 0, 10, 20, 30 and 40 cycles, tubes were removed from the PCR thermocycler and placed in a -20°C freezer.

3.4.3 PCR Purification and Precipitation

In order to eliminate background noise such as primers, enzymes, cellular debris, and salts, PCR purification was performed using a PCR purification kit from Qiagen. The procedure for this kit can be found in the Qiaquick PCR purification manual.

To further purify the amplified DNA and to remove excess salt ions left over from the PCR purification step, an alcohol precipitation procedure was implemented. This procedure followed the same steps as the precipitation technique that was used with the 100, 500, and 5000 base pair DNA samples from Fermentas. The only change was the final resuspension volume was 50µL instead of 75µL.

3.4.4 Micro-scale device design and fabrication

The biochips were provided by BioVitesse, Inc. The fabrication process of the biochip sensor was similar to Gomez, et al. [45] and started with bare 4" silicon wafers, with a (100) surface and a thickness of 500µm. Silicon dioxide was thermally grown on the wafers and subsequently patterned with conventional photolithography (using Clariant AZ1518 positive photoresist, Clariant Corp.,Somerville, NJ) followed by etching in buffered hydrofluoric acid (BHF). This oxide layer serves as a hard mask for etching the channels in an anisotropic potassium-hydroxide-based etchant to a nominal depth of 12µm. After etching the channels, the hard mask was removed by etching in BHF and the wafers were thermally reoxidized to create a 2000-Å layer of silicon dioxide. Subsequently, a metal layer, which creates the measurement electrodes and the RTD temperature sensor, was deposited by sputtering 800 Å of platinum over a titanium adhesion layer (Perkin-Elmer Sputterer Model 2400, Perkin-Elmer Inc., Wellesley, MA) and

patterned by liftoff. Subsequently, a 10,000-Å-thick layer of gold over a titanium adhesion layer was deposited by electron-beam evaporation (Varian Inc., Palo Alto, CA) and patterned by wet etch to create robust bond-pads. After dicing the wafers, a glass cover was anodically bonded to each die at 400 mAmps with a voltage of 1000 V for 60 min. The glass cover was made from 4", 500μm thick polished Pyrex glass wafers type 7740 (Corning Inc., Corning, NY), which were custom diced and ultrasonically drilled to create holes where input/output tubes were attached. The holes in the glass were aligned to the input/output channels in the die before anodic bonding. Fig. 12 (A) shows a cross section of the packaged device.

After fabrication, each die was fixed onto a custom-designed printed circuit board carrier that allows it to be easily connected to the equipment that measures the impedance, and measures and controls the temperature. The carrier contains an integrated heater and gold-plated bond pads that connect to the pads on the chip by wire bonding. Fig. 12 (C) shows a packaged biochip on a pc board.

3.4.5 Impedance measurement

The impedance of each PCR sample was measured by the LCR meter in the BioVitesse System. A DI water curve was taken as a baseline reading before each set of measurements to ensure the system had achieved a consistent baseline measurement to measurement. After DI, 25 μL of sample solution was injected into the chip at a rate of 20μL/min. The measurement voltage was 250 mV_{p-p} with 12 frequencies, 10, 32, 100, 200, 250, 500, 800, 1000, 2500, 5000, 7500, and 10000Hz. 10-12 sweeps were taken for each sample to ensure that the system had stabilized and

was functioning properly. To minimize the issue of DNA contamination between cycle samples. The samples were run from low concentration to high concentration or from 0 cycle to 40 cycle.

3.4.6 PCR Confirmation

As a method of amplification confirmation, gel electrophoresis was run for each cycle sample with a 100bp low ladder from BioRad as the standard. The 100mL gel was made with 1x TE buffer, 1% high purity agarose and 2μL ethidium bromide. The samples were loaded into the wells using a loading dye from BioRad. The gel was then run at 100V for approximately 2 hours. An image of the gel was taken using a GelDoc XR system with a UV illuminator from BioRad.

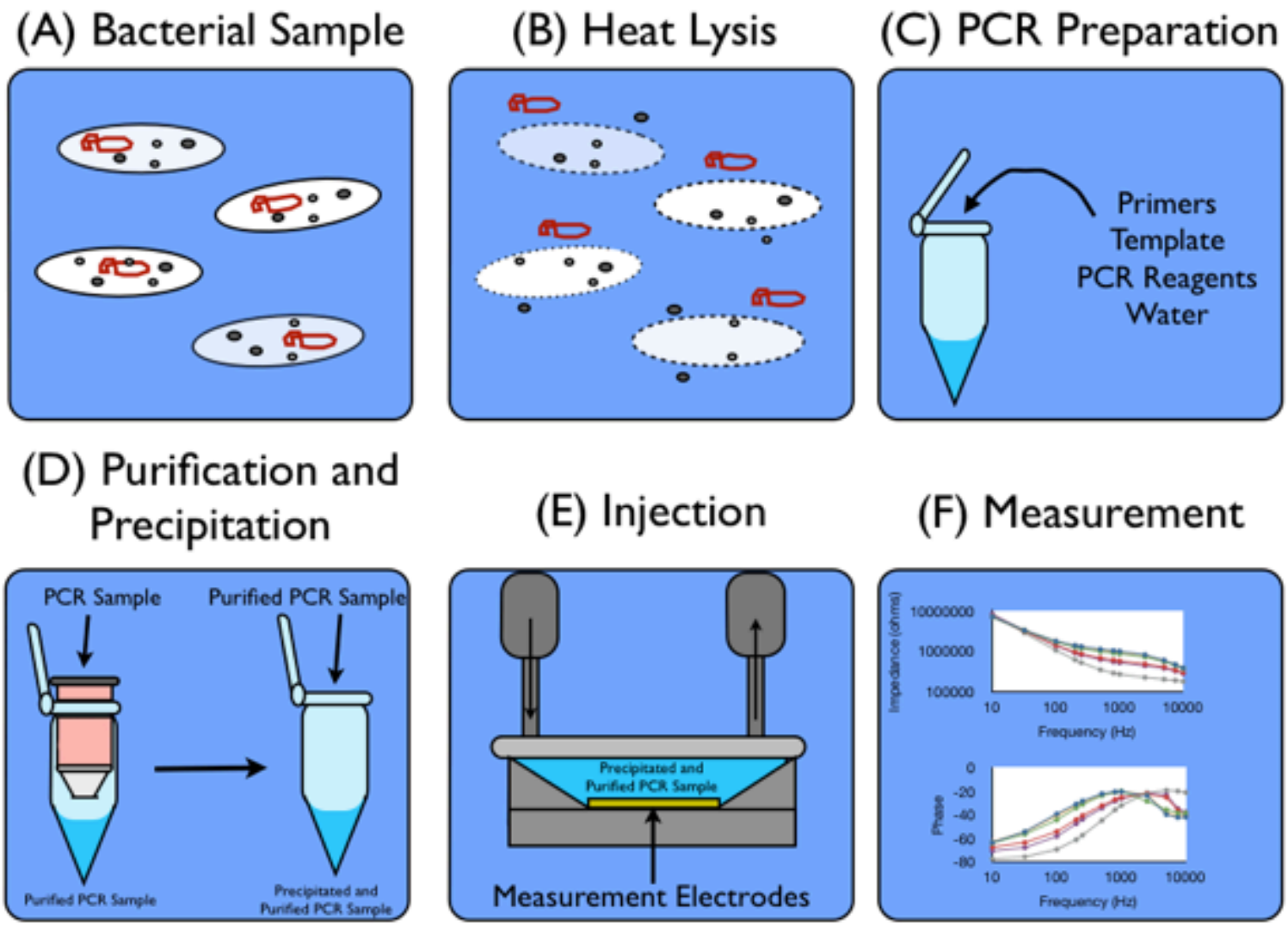

Figure 10: This figure depicts the proposed procedure. (A) Depicts the bacterial culture (B) Depicts cell lysis in preparation for PCR (C) Depicts the PCR reagent, primer and template mixing (D) Depicts the post-thermocycling purification and precipitation of the PCR product (E) Depicts injection the sample into the BioVitesse chip (F) Depicts the impedance spectroscopy measurements and subsequent impedance and phase results from a sample.

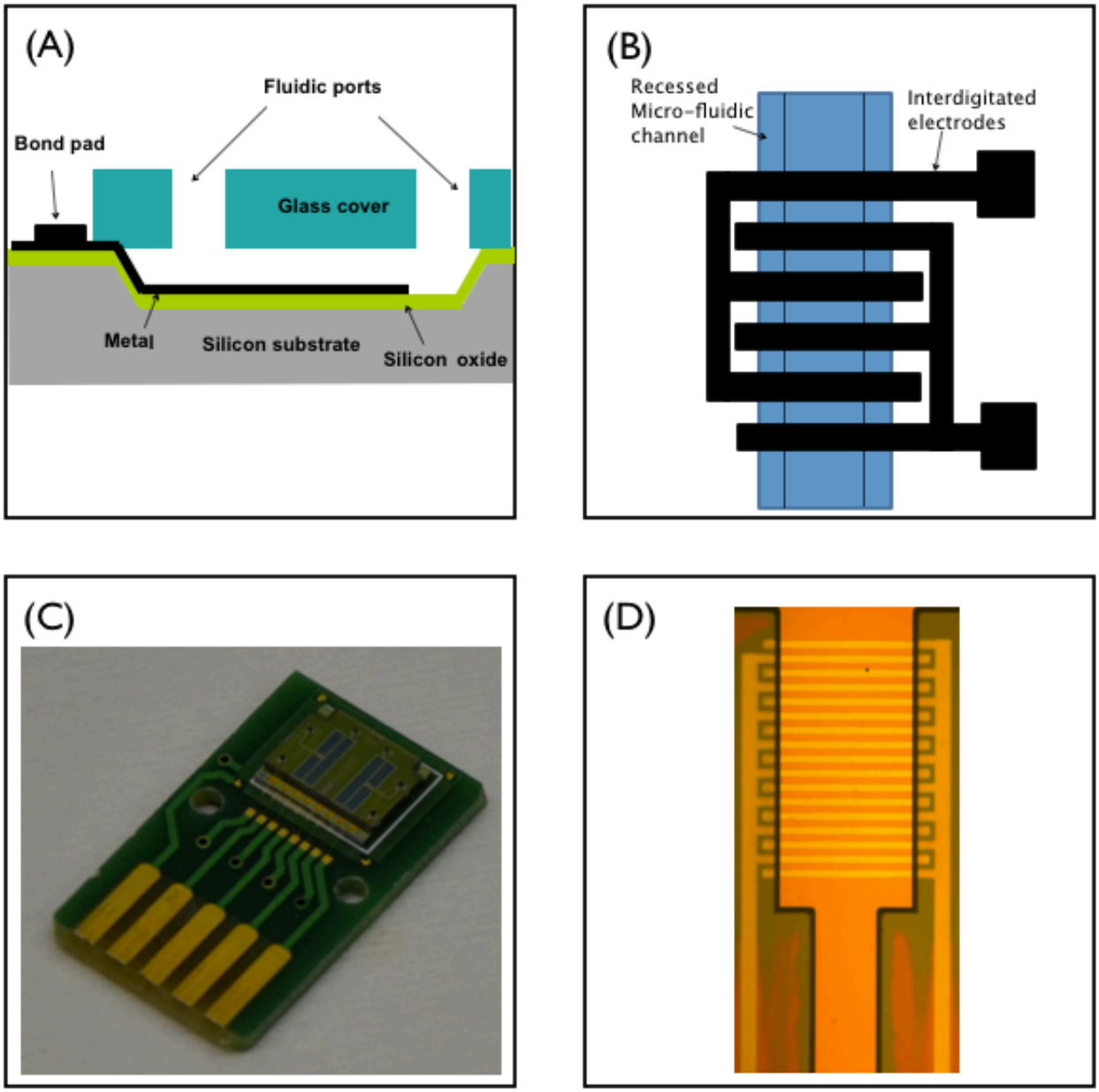

Figure 11: (A) A cross-sectional view of the microchip is show. The portion containing the interdigitated electrodes comprises a volume of 60nL. (B) A top view of the sensing region is shown. (C) The whole chip is shown. Inlet and outlet ports are visible, as well as a secondary sensing chamber that can be used as a reference well. (D) A photograph of the sensing region is shown.

3.5 Results/Discussion

3.5.1 Varying DNA molecule length and concentration in DI water

The impedance spectroscopy plots for the 100, 500, and 5000bp samples from Fermentas are shown in Figure 12. It can be seen that as the concentration of DNA molecules increases for 100, 500, and 5000 bp, the impedance decreases and the dielectric relaxation point shifts to higher frequencies.

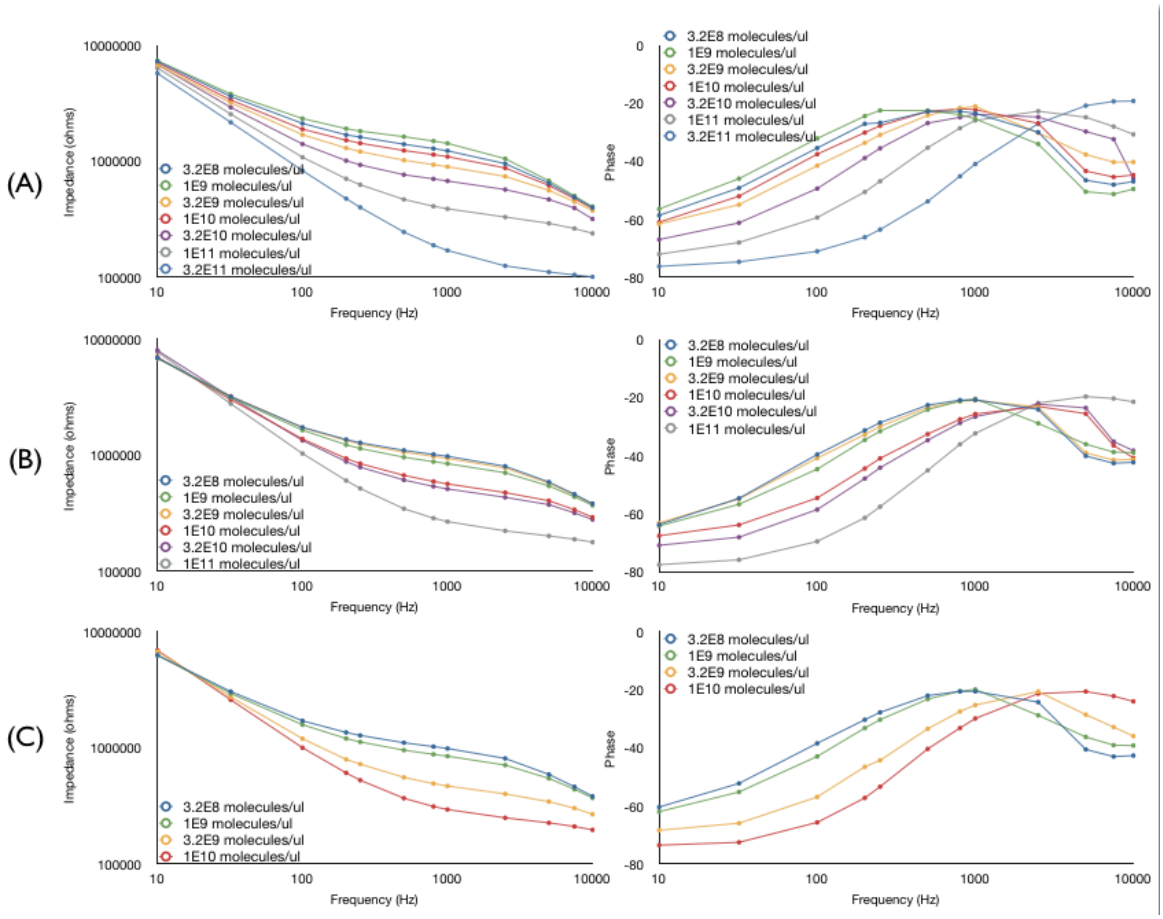

Figure 12: Pure DNA samples diluted in nuclease free DI water were tested. The above figure shows (A) 100, (B) 500, and (C) 5000bp DNA fragments as they were interrogated from 10Hz-10kHz. Changes in phase and impedance can be seen with changing DNA concentration.

The change in impedance is likely due to the increase number of molecules in solution and the resulting change in capacitance and conductivity. The shifting phase change is more difficult to understand. As the number of molecules increases, the dielectric relaxation point shifts to higher and higher frequencies. This implies that the time it takes for the dipole formation and alignment is taking a shorter and shorter amount of time. There are two likely reasons for this phenomenon. For DNA strands whose length is above the persistence length of the DNA in solution (50-100nm), the subunit length of the DNA molecule will decrease with increasing solution conductivity and salt concentration [46]. In Figure 13 (A), the increase in the conductivity of the solution can also be seen in the changing impedance values for the different length DNA molecules at 1 kHz. As this subunit length decreases, the degree of coiling of the DNA molecule will increase. This leads to a decreased effective length of the molecule which will allow the counter-ion cloud and dipole alignment to occur at higher frequencies. A secondary effect arises from the changing concentration of DNA. Dobrynin and Rubinstein were able to show that the number of condensed counter-ions increases with increasing polyelectrolyte concentration [47]. As the number of condensed counter-ions increases, electrostatic interactions in the DNA chain are weakened. Weakening of the repulsive forces between negatively-charged phosphate groups causes shrinkage in the polyelectrolyte chain. By reducing the size of the polyelectrolyte chain, counter-ion cloud and dipole alignment can happen at a quicker rate which shifts the relaxation point to a higher frequency, a result that is repeated in our work and is especially applicable to the 100bp sample whose chain length is less than the average persistence length of DNA.

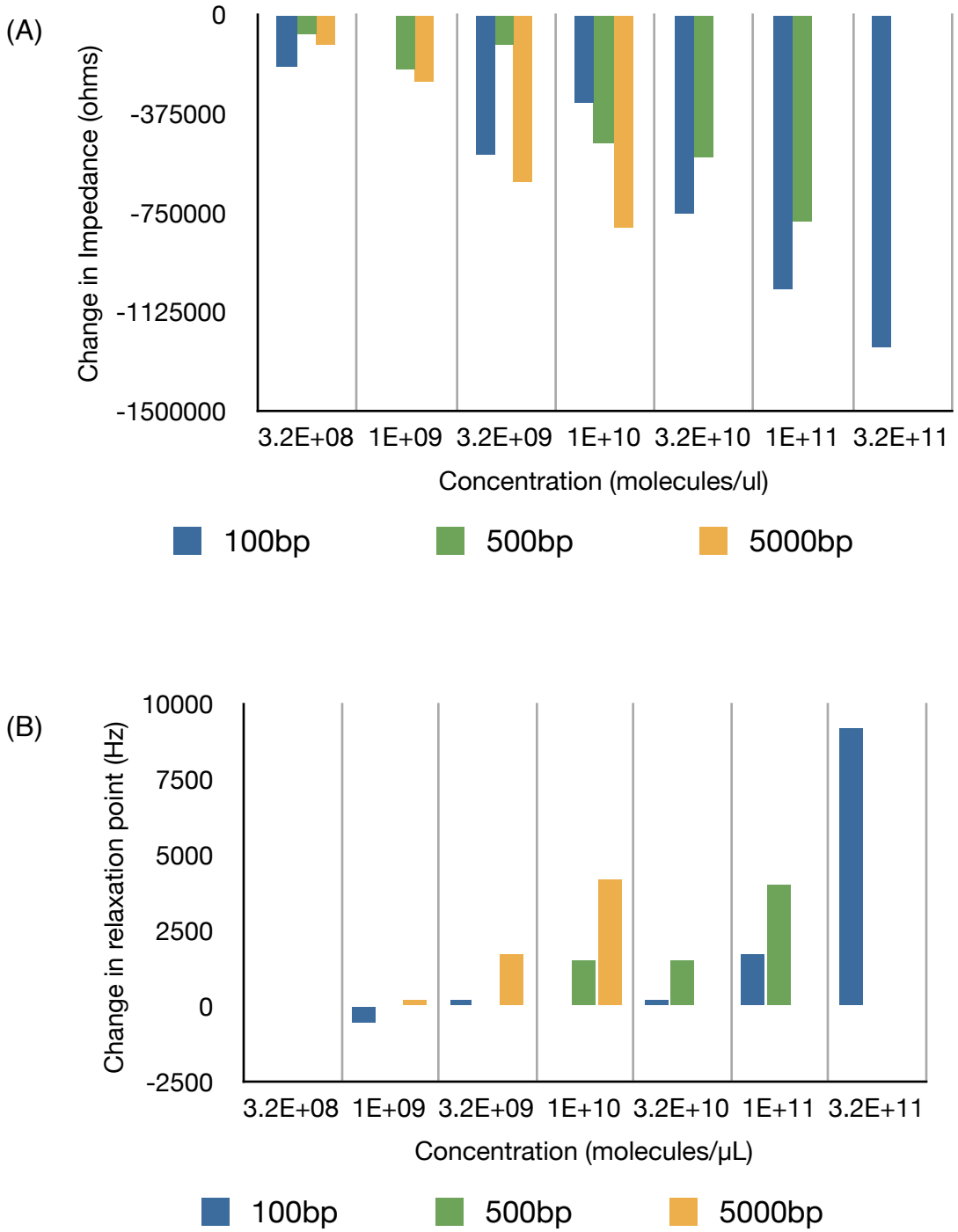

Figure 13: The change in impedance at 1 kHz referenced to a DI sample is shown. It can be seen that the change in impedance shows concentration dependence within each sample. Between each sample it can be seen that there exists a dependence on molecular weight. At a certain concentration of molecules, the change in impedance increases relative to increasing molecular weight. This is most clearly seen at the concentration of 1E10 molecules/ul.

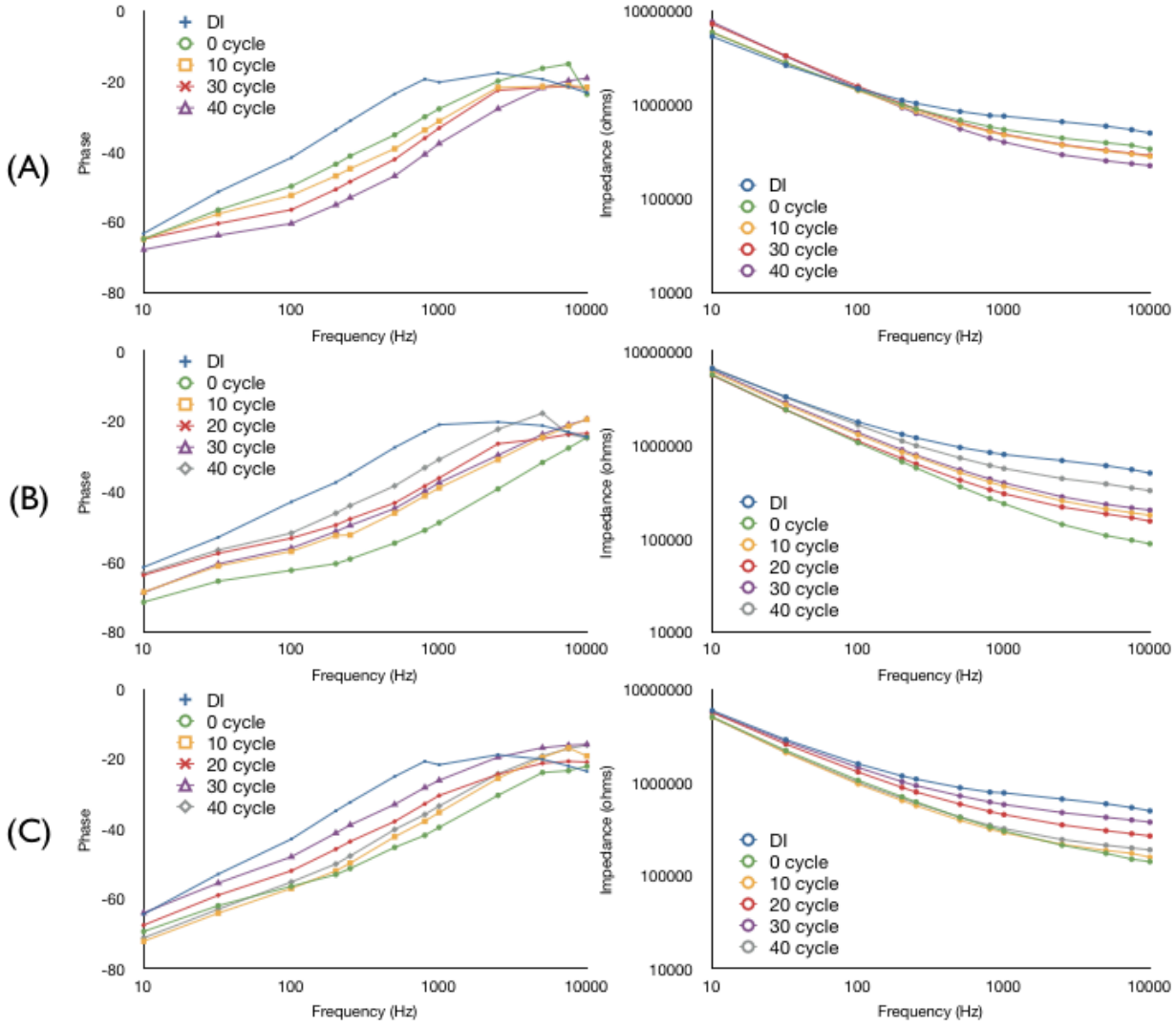

Figure 14: Purified PCR samples were tested over a range of 10 Hz-10 kHz. The impedance and phase response is charted for (A) a full PCR test, (B) a primer only test, and (C) a template only test. In each test, different thermocycling points ranging from 0 cycles up to 40 cycles, are measured in order to monitor the change in impedance and phase relative to target DNA concentration.

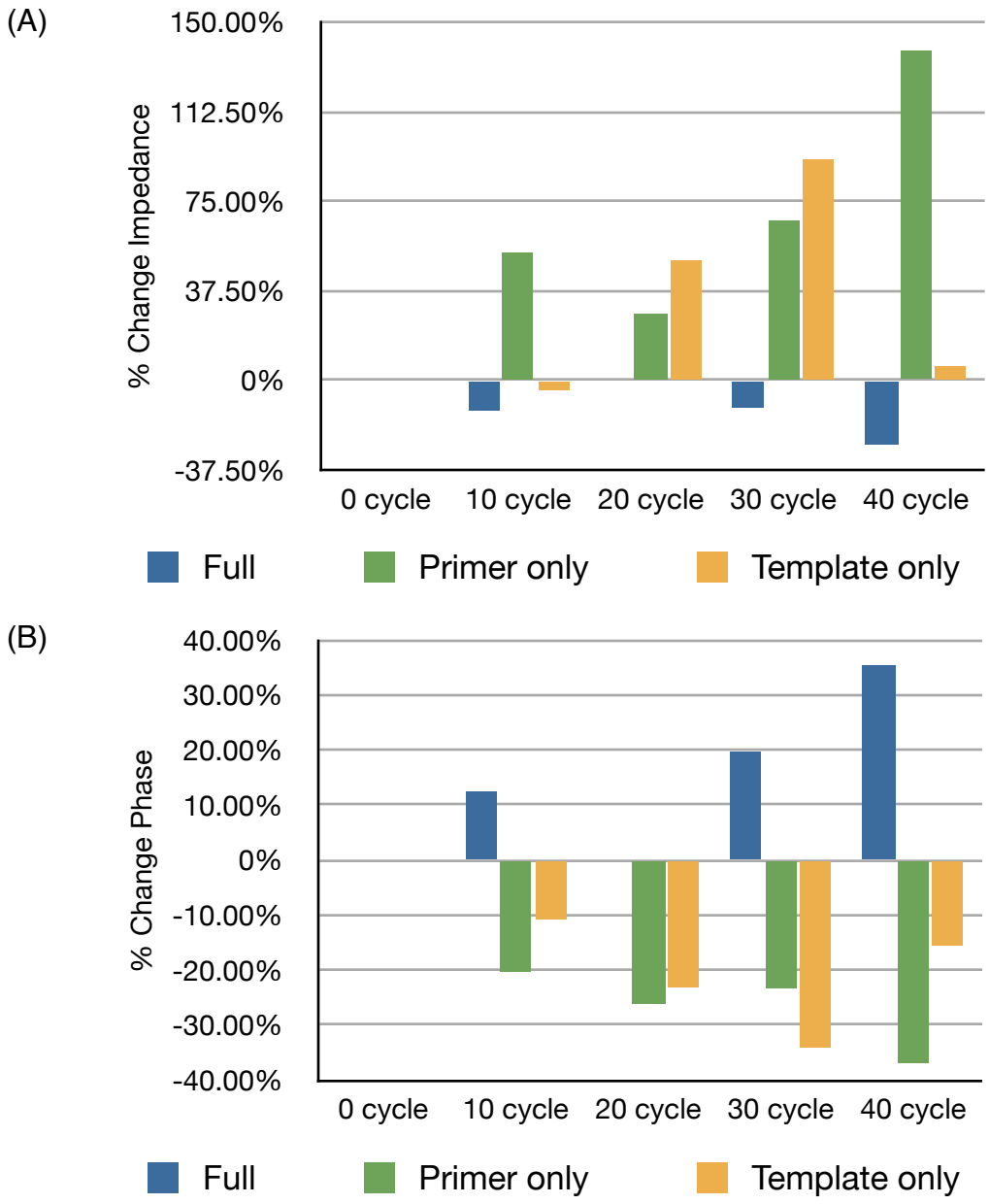

Figure 15: The percent change in impedance (A) and phase (B) are plotted with respect to the 0 cycle measurement.

3.5.2 Detection of PCR amplification

After establishing the detection limit of dsDNA molecules in DI water, we applied the label-free impedance spectroscopy method to detection of PCR amplification. In order to minimize the

effects of charge shielding, ion binding, and variance in ion composition, the amplified PCR product was first purified to remove primers and PCR reagents and then precipitated out of solution and resuspended in DI water in order to remove excess salt ions.

Figure 14 shows the raw data from one of the sample runs. A clear increase in the relaxation maxima with increasing cycle number for the positive PCR sample can be seen in the raw data. As confirmed through gel electrophoresis and nanodrop spectrophotometery (data not shown), the 30 and 40 cycle samples contain roughly 3E10 508bp molecules/µl and 1E11 508bp molecules/µl respectively. This is similar to the two highest 500bp concentrations studied in the dsDNA test from Figure 12 (B). Results from the full PCR test are consistent with the 500bp dsDNA test. To confirm the increase in relaxation maxima in the phase is solely due to the amplified PCR product, negative controls were run. The primer only sample shows no increase in relaxation maxima and no decrease in impedance from 0 to 40 cycles. The same can be said of the sample containing template only. A change in the opposite direction from the full PCR sample from 0 to 40 cycles was seen in both negative controls. This is believed to be an artifact of the thermal cycling process and the purification and precipitation technique, however the exact reasoning for this change is unknown. The trend for the full PCR sample follows expectations and is considered significant and repeatable. Figure 15 looks at the relative changes in phase and impedance for the raw data. The data shows a large increase in phase and a decrease in impedance for the full PCR sample. This is a similar trend to the 500bp sample data from Figure 12 (B). However, in this plot, the relative change from the 0 cycle measurement is plotted. This provides a view of how the system changes from 0 to 40 cycles.

In practice, the samples from the environment will not contain just one type of microorganism. Therefore, in order to prove a method that works well for the detection of food-borne pathogens, selectivity experiments of one specific bacterium from a mixture of microorganisms would also have to be examined. Additionally, the effects of culturing pathogens from a food matrix would also have to be investigated.

3.6 Conclusions

This study details the initial stages of development of a label-free, PCR biosensor capable of detecting changing DNA concentration. While the current detection limit of this system is relatively high, in the 30-40 cycle range, further development of the system could put its capabilities on par with current real-time PCR detection devices. Amplifying the signal from the DNA molecules is a strong possibility for improvement. This can either be done through concentration of the DNA at the electrode surface through a technique such as dielectrophoresis [48] or through inclusion of negatively DNA binders [49]. Overall, this study has laid down the basis for a label-free detection method for PCR. In the future, this technique could be incorporated into a lab-on-a-chip device and used as a point-of-care diagnostic device for the food industry or for medical applications.

Chapter 4. Conclusions

4.1 Overview of Accomplished Goals

The development of more cost-efficient, reliable food-borne pathogen detection methods will enable food companies to provide safer food, faster at a more affordable cost to the consumer. To that end, this study details the methods used to minimize the cost and time of two of the most common types of food-borne pathogen detection systems.

By removing the need for enzyme-linked secondary antibodies, the presented photonic crystal-based label-free biosensor advances the field of immunoassays for bacterial detection. By removing the need for fluorescent dyes in real-time PCR, the presented label-free detection method greatly improves the practicality of a point-of-care pathogen diagnostic system.

4.2 Future Prospects

In order to further develop the photonic crystal system, optimization of the blocking agent as well as further specificity tests would have to be completed. Additionally, the detection limit of the system would have to be increased. An option for increasing the detection limit of this sort of system is to incorporate solution flow. By flowing a larger volume over the sensor, a greater number of antigens will interact with the antibodies. Incorporation of dielectrophoresis(DEP) is another possibility. If the sensor is made thin enough, a dielectrophoretic setup could be placed under the photonic crystal. By using DEP, cells or antigens could be pulled down out of solution

and concentrated at the sensor surface [50]. This may help minimize the problems of limited cellular diffusion in a microwell.

The electrical detection of PCR protocol must also be improved. Real-time PCR techniques show a detection limit closer to the 20 cycle range instead of the 40 cycle range. This is another setup that could benefit from DEP. DEP has been shown to concentrate DNA at the surface of electrodes. Increasing the local concentration of DNA molecules by 10 fold would mean that the system would be able to detect 1E10 molecules/µl. In a PCR reaction, it is feasible to achieve this sort of yield by 20-25 cycles. Another key component to enhance in this system would be to limit off chip procedures. Scientists have shown systems that integrate PCR purification into a microfluidic device [51-54]. By combining an on-chip thermocycling process and a PCR purification step within the chip's own microfluidics with electrical detection of DNA molecules, an on-site diagnostic system with limited cost and footprint is possible.

In further developing label-free biosystems designed for the food industry, this report has hopefully brought cheaper, faster, smaller biosensors one step closer to reality.

References

1. "CDC - Estimates of Foodborne Illness Questions and Answers." Centers for Disease Control and Prevention. Web. 03 Apr. 2011. <http://www.cdc.gov/foodborneburden/questions-and-answers.html>.

2. "ERS/USDA Data Foodborne Illness Cost Calculator." USDA Economic Research Service - Home Page. Web. 03 Apr. 2011. <http://www.ers.usda.gov/data/foodborneillness/>.

3. Crutchfield, Stephen R., and Tanya Roberts. "Food Safety Efforts Accelerate in the 1990's." Food Review Vol. 23, No. 3, p.44-49, 2000.

4. "Response to Questions Posed by the Food Safety and Inspection Service Regarding Determination of the Most Appropriate Technologies for the Food Safety and Inspection Service To Adopt in Performing Routine and Baseline Microbiological Analyses." Journal of Food Protection, Vol. 73, No. 6, p.1160–1200, 2010.

5. "AOAC International | Rapid Test Kits | Performance Tested Methods | List of Tested Methods." AOAC INTERNATIONAL Homepage. Web. 03 Apr. 2011. <http://www.aoac.org/testkits/testedmethods.html>.

6. "Bacteriological Analytical Manual (BAM)." U S Food and Drug Administration Home Page. Web. 03 Apr. 2011. <http://www.fda.gov/Food/ScienceResearch/LaboratoryMethods/BacteriologicalAnalyticalManualBAM/default.htm>.

7. Higuchi, Russell, Gavin Dollinger, P. Sean Walsh, and Robert Griffith. "Simultaneous Amplification and Detection of Specific DNA Sequences." Bio/Technology 10.4, p.413-17. 1992.

8. Higuchi, Russell, Carita Fockler, Gavin Dollinger, and Robert Watson. "Kinetic PCR Analysis: Real-time Monitoring of DNA Amplification Reactions." Bio/Technology 11.9, p.1026-030, 1993.

9. Lock, K., D. Stuckler, K. Charlesworth, and M. McKee. "Potential Causes and Health Effects of Rising Global Food Prices." Bmj 339.Jul13 1, B2403, 2009.

10. Joannopoulos, John D., Steven G. Johnson, Joshua N. Winn, and Robert David Meade. Photonic Crystals: Molding the Flow of Light. 2nd ed. Princeton, NJ: Princeton UP, 2008.

11. M.F. Pineda, L.L. Chan, T. Kuhlenschmidt, M. Kuhlenschmidt, and B.T. Cunningham. "Rapid label-free selective detection of porcine rotavirus using photonic crystal biosensors," IEEE Sensors Journal, Vol. 9, No. 4, p.470-477, 2009.

12. Lin, B., J. Pepper, P. Li, H. Pien, and B.T. Cunningham "A Label-Free High Throughput Optical Technique for Detecting Small Molecule Interactions." Biosensors and Bioelectronics, Vol. 17, No. 9, p. 827-834, 2002.

13. Chan, L., S. Gosangari, K. Watkin, and B.T. Cunningham. "A label-free photonic crystal biosensor imaging method for detection of cancer cell cytotoxicity and proliferation." Apoptosis, Vol. 12, No, 6, p. 1061-1068, 2007.

14. Chan, L.L., E.A. Lidstone, K.E. Finch, J.T. Heeres, P.J. Hergenrother, and B.T. Cunningham. "A method for identifying small molecule aggregators using photonic crystal biosensor microplates." Journal of the Association for Laboratory Automation (JALA), Vol. 14, No. 6, p.348-359, 2009.

15. Choi, C. J., I.D. Block, B. Bole, D. Dralle, B.T. Cunningham."Photonic Crystal Integrated Microfluidic Chip for Determination of Kinetic Reaction Rate Constants." IEEE Sensors Journal, Vol. 9, No. 12, p. 1697-1704, 2009.

16. Heeres, J.T., S.-H. Kim, B.J. Leslie, E.A. Lidstone, B.T. Cunningham, and P.J. Hergenrother. "Identifying modulators of protein-protein interactions using photonic crystal biosensors." Journal of the American Chemical Society, Vol. 131, No. 51, p.18202-18203, 2009.

17. Wu, Chia-Chen, Sara D. Alvarez, Camilla U. Rang, Lin Chao and Michael J. Sailor, "Label-free optical detection of bacteria on a 1-D photonic crystal of porous silicon", Proc. SPIE 7167, 71670Z, 2009.

18. "Product Catalog: Antibodies and Substrates for ELISA, Blotting, Immunohistochemistry." KPL- See More with KPL Protein Detection and Analysis Tools. Web. 04 Apr. 2011. <http://www.kpl.com/catalog/productdetail.cfm?catalog_id=17>.

19. Taylor, A., Q. Yu, S. Chen, J. Homola, and S. Jiang. "Comparison of E. Coli O157:H7 Preparation Methods Used for Detection with Surface Plasmon Resonance Sensor." Sensors and Actuators B: Chemical 107.1, p.202-08. 2005.

20. Saiki, R., D. Gelfand, S. Stoffel, S. Scharf, R. Higuchi, G. Horn, K. Mullis, and H. Erlich. "Primer-directed Enzymatic Amplification of DNA with a Thermostable DNA Polymerase." Science 239.4839, p. 487-91, 1988.

21. Northrup, M.A., M. T. Ching, R. M. White, R. T. Wltson, "DNA amplification with a microfabricated reaction chamber," Proceedings of Transducers '93, p.924-926, 1993.

22. Lagally, E. T., I. Medintz, and R. A. Mathies, "Single-Molecule DNA Amplification and Analysis in an Integrated Microfluidic Device," Anal. Chem., vol. 73, p.565-570, Feb. 2001.

23. Khandurina, J.m T. E. McKnight, S. C. Jacobson, Larry C. Waters, R. S. Foote, and J. Michael Ramsey, "Integrated System for Rapid PCR-Based DNA Analysis in Microfluidic Devices," Anal. Chem., vol. 72, p. 2995-3000, 2000.

24. El-Ali, J., I. R. Perch-Nielsen, C. R. Poulsen, D. D. Bang, P. Telleman, A. Wolff, "Simulation and experimental validation of a SU-8 based PCR thermocycler chip with integrated heaters and temperature sensor," Sensors and Actuators A, vol. 110, p.3-10, 2004.

25. Liao, Chia-Sheng, G.B. Lee, J.J. Wu, C.C. Chang, T-M. Hsieh, F-C. Huang, and Ching-Hsing Luo, "Micromachined polymerase chain reaction system for multiple DNA amplification of upper respiratory tract infectious diseases," Biosensors and Bioelectronics, vol. 20, p.1341-1348, 2005.

26. Ke, Cathy, A-M Kelleher, H. Berney, M. Sheehan, Alan Mathewson, "Single step cell lysis/PCR detection of Escherichia coli in an independently controllable silicon microreactor," Sensors and Actuators B, vol. 120, p.538-544, 2007.

27. Bhattacharya, S., S. Salamat, D. Morisette, P. Banada, D. Akin, Y-S. Liu, A.K. Bhunia, M. Ladisch, and Rashid Bashir, "PCR-based detection in a micro-fabricated platform," Lab Chip, vol. 8, p.1130-1136, 2008.

28. Woolley, Adam T., D. Hadley, P. Landre, A. J. deMello, R. A. Mathies, and M. Allen Northrup, "Functional Integration of PCR Amplification and Capillary Electrophoresis in a Microfabricated DNA Analysis Device," Anal. Chem., vol. 68, p.4081-4086, 1996.

29. Waters, Larry C., S.C. Jacobson, N. Kroutchinina, J. Khandurina, R.S. Foote, and J. Michael Ramsey, "Multiple Sample PCR Amplification and Electrophoretic Analysis on a Microchip," Anal. Chem., vol. 70, p.5172-5176, 1998.

30. Huang, Fu-Chun, C-S. Liao, Gwo-Bin Lee, "An integrated microfluidic chip for DNA/RNA amplification, electrophoresis separation and on-line optical detection," Electrophoresis, vol. 27, p.3297-3305, 2006.

31. Cady, Nathaniel C., S. Stelick, M.V. Kunnavakkam, Carl A. Batt, "Real-Time PCR detection of Listeria monocytogenes using and integrated microfluidics platform," Sensors and Actuators B, vol. 107, p.332-341, 2005.

32. Wang, Jing, Z. Chen, P. L. A. M. Corstjens, M.G. Mauk, and Haim H. Bau. "A Disposable Microfluidic Cassette for DNA Amplification and Detection." Lab on a Chip 6.1, p46-53, 2006.

33. Zhang, G., Zhang, L., Huang, M. J., Luo, Z. H. H., Tay, G. K. I., Lim, E. A. Kang, T.G., Chen, Y. "Silicon nanowire biosensor for highly sensitive and rapid detection of dengue virus". Sensors and Actuators, B: Chemical, 146(1), p138-144, 2010.

34. Ghindilis, Andrei L., Maria W. Smith, Kevin R. Schwarzkopf, Changqing Zhan, David R. Evans, António M. Baptista, and Holly M. Simon. "Sensor Array: Impedimetric Label-Free Sensing of DNA Hybridization in Real Time for Rapid, PCR-Based Detection of Microorganisms." Electroanalysis 21.13, p.1459-1468, 2009.

35. Henry, O.Y.F., J.L. Acero Sanchez, D. Latta, and C.K. O'Sullivan. "Electrochemical Quantification of DNA Amplicons via the Detection of Non-hybridised Guanine Bases on Low-density Electrode Arrays." Biosensors and Bioelectronics 24.7, p.2064-2070, 2009.

36. Mandel, M. "The Electric Polarization of Rod-like, Charged Macromolecules." Molecular Physics 4.6, p. 489-96, 1961.

37. Takashima, Shiro. "Dielectric Dispersion of Deoxyribonucleic Acid. II." Journal of Physical Chemistry 70 (5), pp. 1372-1380, 1966.

38. Jerrard, H. G. and B.A. W. Simmons. "Dielectric Studies on Deoxyribonucleic Acid." Nature 184, p.1715 - 1716, 1959.

39. Sakamoto, Masanori, H. Kanda, R. Hayakawa, and Yasaku Wada. "Dielectirc Relaxation of DNA in Aqueous Solutions." Biopolymers 15.5, p.879-892, 1976.

40. Oosawa, Fumio. "Counterion Fluctuation and Dielectric Dispersion in Linear Polyelectrolytes." Biopolymers 9.6, 677-688, 1970.

41. Mandel, M., and T. Odijk. "Dielectric Properties of Polyelectrolyte Solutions." Annual Review of Physical Chemistry 35.1, 75-108, 1984.

42. Takashima, S. "Dielectric Behavior of DNA Solution at Radio and Microwave Frequencies (at 20 Degrees C)." Biophysical Journal 46.1, p.29-34, 1984.

43. Tomić, S., S. Dolanski Babić, T. Vuletić, L. Griparić, and R. Podgornik. "Dielectric Relaxation of DNA Aqueous Solutions." Physical Review E 75.2, art. no. 021905, 2007.

44. Liu, Yi-Shao, Padmapriya P. Banada, Shantanu Bhattacharya, Arun K. Bhunia, and Rashid Bashir. "Electrical Characterization of DNA Molecules in Solution Using Impedance Measurements." Applied Physics Letters 92.14, 143902, 2008.

45. R. Gomez, R. Bashir, T. Geng, A. Bhunia, M. Ladisch, H. Apple, S. Wereley, "Micro-Fluidic Bochip for Impedance Spectroscopy of Biological Species", Biomedical Micro-Devices, vol. 3, no. 3, p. 201-209, 2001.

46. Hagerman, Paul J. "Flexibility of DNA." Annual Review of Biophysics and Biophysical Chemistry 17.1, p.265-86, 1988.

47. Dobrynin, A., and M. Rubinstein. "Theory of Polyelectrolytes in Solutions and at Surfaces." Progress in Polymer Science 30.11, p.1049-1118, 2005.

48. Asbury, C. L., Diercks, A. H. and van den Engh, G., "Trapping of DNA by dielectrophoresis". Electrophoresis, 23: 2658–2666, 2002.

49. Kafka, J., O. Panke, B. Abendroth, and F. Lisdat. "A Label-free DNA Sensor Based on Impedance Spectroscopy." Electrochimica Acta 53.25, p.7467-7474, 2008.

50. Park, Kidong, H. Suk, D. Akin and R. Bashir "Dielectrophoretic-based cell manipulation using electrodes on reusable printed circuit board", Lab Chip, 9, p.2224 - 2229, 2009.

51. Wolfe, KA and Breadmore, MC and Ferrance, JP and Power, ME and Conroy, JF and Norris, PM and Landers, JP. "Toward a microchip-based solid-phase extraction method for isolation of nucleic acids". Electrophoresis, 23 (5). p.727-733, 2002.

52.Wen, Jian, Lindsay A. Legendre, Joan M. Bienvenue, and James P. Landers. "Purification of Nucleic Acids in Microfluidic Devices." Analytical Chemistry 80.17, p.6472-6479, 2008.

53. Junhong Min, Junhong, Kim,J-H., Lee, Y., Namkoong, K., Im, H-C., Kim, H-N., Kim, H-Y., Huh, N. and Young-Rok Kim. "Functional Integration of DNA Purification and Concentration into a Real Time Micro-PCR Chip." Lab on a Chip, 11, p.259-265, 2011.

54. Cady, Nathaniel C., Stelick, S. and Carl A. Batt. "Nucleic Acid Purification Using Microfabricated Silicon Structures." Biosensors and Bioelectronics 19.1, p.59-66, 2003.